

# POTENTIAL FLOW SOLUTION FOR A YAWED SURFACE-PIERCING FLAT PLATE

Hongbo Xu and J.N. Newman  
Department of Ocean Engineering, MIT, Cambridge, Mass., U.S.A.

## Introduction

The analysis of the flow past a lifting surface of zero thickness is essential in many potential flow problems with or without the presence of a free surface. Classic examples are the thin wing theory and the problem of a yawed surface-piercing plate. In the absence of a free surface, the Vortex-Lattice Method (VLM) gives accurate results for the aerodynamic characteristics of a flat airfoil. The numerical results for some typical lifting planforms can be found in works by Garner et al (1968) and Lan (1974). Newman (1961) derived an integral equation formulation for a rectangular surface-piercing plate. Daoud (1973) attempted to solve the integral equation numerically, but the numerical scheme didn't converge. Chapman (1976) used the slender-body approximation to solve the same problem, however, the effects of transverse waves were not included. This paper presents a boundary element method for the solution of the problem of a yawed rectangular surface-piercing flat plate.

## Formulation

A uniform free-surface flow of velocity  $U$  past a flat plate at a small angle of attack  $\alpha$  is considered. It is assumed that the flow is incompressible and irrotational except for a sheet composed of the lifting surface and its wake. It follows that the potential  $\phi$  satisfies the Laplace equation in the fluid domain  $V$ :

$$\nabla^2 \phi = 0 \quad (1)$$

the body boundary condition on the linearized body surface  $S_b$ :

$$\frac{\partial \phi}{\partial \mathbf{y}} = \mathbf{U} \cdot \mathbf{n} \quad (2)$$

where  $\mathbf{n}$  is the unit normal vector on  $S_b$ ; the linearized free surface condition:

$$\frac{\partial^2 \phi}{\partial x^2} - \frac{g}{U^2} \frac{\partial \phi}{\partial y} = 0 \quad (3)$$

on  $y = 0$  or  $S_f$ ; a bottom condition:

$$\frac{\partial \phi}{\partial y} = 0 \quad \text{as } y \rightarrow \infty \quad (4)$$

and a radiation condition at infinity. In addition it is necessary to impose the Kutta condition at the trailing edge, and the condition that the pressure is continuous across the wake  $S_w$ . Defining a field point  $p = (x, y, z)$  and a unit singularity point  $q = (\xi, \eta, \zeta)$ , the Green function corresponding to the above boundary value problem can be written as

$$G(p, q) = \frac{1}{r} - \frac{1}{r_0} + H(p, q) \quad (5)$$

where  $r$  and  $r_0$  are, respectively, the distances from a field point to the singularity point and its image above the free surface, and the  $H$  function represents the free surface effects. Using the Green's formula:

$$\iint_{\forall S} \left( G \cdot \frac{\partial \phi}{\partial \mathbf{n}} - \frac{\partial G}{\partial \mathbf{n}} \cdot \phi \right) ds = \begin{cases} 4\pi\phi(p) & \text{if } p \in V; \\ 2\pi\phi(p) & \text{if } p \text{ on } S_b; \\ 0 & \text{elsewhere.} \end{cases} \quad (6)$$

and applying the boundary conditions on the free surface, the bottom, and at infinity, the potential  $\phi$  is readily expressed by

$$\phi(p) = -\frac{1}{4\pi} \iint_{S_b \cup S_w} [\phi(\xi, \eta, 0^+) - \phi(\xi, \eta, 0^-)] \frac{\partial G}{\partial n} ds \quad (7)$$

Letting  $m(\xi, \eta) = \phi(\xi, \eta, 0^+) - \phi(\xi, \eta, 0^-)$ , and imposing the boundary condition on the body surface, we obtain

$$-\frac{1}{4\pi} \lim_{z \rightarrow 0} \frac{\partial}{\partial z} \iint_{S_b \cup S_w} m(\xi, \eta) \frac{\partial G}{\partial n} d\xi d\eta = \mathbf{U} \cdot \mathbf{n} \quad (8)$$

which is an integral equation of the first kind for  $m(\xi, \eta)$ . From equation (7), the potential of the flow is expressed in terms of the unknown dipole strength distributed over the lifting surface and its wake, which can be found by solving equation (8). As indicated by Burton (1971), the difficulties sometimes associated with this type of integral equations do not arise with equation (8) to any marked degree because of the singularity of the kernel at  $p = q$ . In the present work, the solvability of the integral equation is considered by studying the corresponding linear system of equations.

### Numerical solutions

To solve equation (8) numerically, the domain of the lifting surface and its wake is discretized into quadrilateral panels with constant dipole strength. Imposing the conditions at the trailing edge and the wake, the unknown dipole strength in the wake can be related to those within the lifting surface  $S_b$ . Thus, no collocation points were introduced over the wake surface  $S_w$ . If the lifting surface and its wake are divided into  $M$  sections vertically, and  $N + N_w$  segments longitudinally, the discrete form of the integral equation is

$$\begin{aligned} & \frac{1}{4\pi} \sum_{j=1}^M \left[ \sum_{i=1}^N m_{ji} \lim_{z \rightarrow 0} \frac{\partial}{\partial z} \iint_{\Delta S_{ji}} \frac{\partial}{\partial \zeta} G(p_l; q_{ji}) d\xi d\eta \right. \\ & \left. + \sum_{i=N+1}^{N+N_w} m_{jN} \lim_{z \rightarrow 0} \frac{\partial}{\partial z} \iint_{\Delta S_{ji}} \frac{\partial}{\partial \zeta} G(p_l; q_{ji}) d\xi d\eta \right] = (\mathbf{U} \cdot \mathbf{n})_l \end{aligned} \quad (9)$$

where  $l = 1 \cdots N_t$ .  $N_t = M \times N$  is the total number of collocation points on the lifting surface. Equation (9) can be written in a standard form of a linear system of equations:

$$[A]\{m\} = \{b\} \quad (10)$$

where  $[A]$  is a  $N_t \times N_t$  influence coefficient matrix.  $\{m\}$  is the  $N_t$ -vector of unknowns.  $\{b\}$  is a known  $N_t$ -vector.

Unlike the VLM formulation, the solution of equation (8) does not have the square-root-type of singularity at the edges. However, the singularity in the kernel of equation (9) should be accounted for carefully. Several different ways of discretizing the lifting surface were examined and compared. For different forward speeds, three cases were considered:

#### (i) The Zero Froude Number Limit:

When the forward velocity is vanishing ( $F_n \rightarrow 0$ ), the linearized free surface boundary condition tends to  $\partial\phi/\partial y = 0$ . The Green function becomes  $G(p, q) = 1/r + 1/r_0$ . This limiting case is equivalent to a lifting surface of twice the aspect ratio moving in an unbounded fluid domain. Thus, the results of this limit case are comparable with those obtained by VLM for the same platform.

#### (ii) The Infinte Froude Number Limit:

If the forward velocity is infinite, the free surface boundary condition becomes  $\phi = 0$ . The Green function becomes  $G(p, q) = 1/r - 1/r_0$ . In this case there is an image lifting surface above the free surface with a negative angle of attack of the same magnitude.

### (iii) The Finite Froude Number Case:

In this case, the Green function takes its general form, i.e. a Rankine pair, a double integral which represents a symmetrical non-radiating disturbance, and a single integral which accounts for the far field waves. In order to evaluate the influence coefficient matrix  $[A]$  in this formulation, the transverse derivative of the Green function is needed. Based on the analysis of Newman (1987a,b), the evaluation of the derivatives were derived and programmed with an estimated accuracy of 5 significant digits.

To ensure the accuracy and dependability of the numerical results, the condition number of the linear system of equations was evaluated, and the convergence of the numerical solutions was examined by either of the two criteria, (1) by refining the grid mesh, the solution should converge to the same limit for a given Froude number; (2) the agreement of the near field and the far field induced drags. For zero and infinite Froude number cases, both criteria were used. However, for simplicity, only the first criterion was employed in the finite Froude number case.

### Results and Conclusions

For the zero Froude number case, the numerical results of the present methods show quantitative agreement with the results by VLM. The convergence of solutions is improved in comparison with that of a conventional VLM. For the infinite Froude number case, results also converge. For the finite Froude number case, a lifting surface of aspect ratio of 0.5 is selected to do the test computation. The lift force coefficients show qualitative agreement with the experimental results reported by Van Den Brug (1971). The numerical solutions converge at high panel density (For the test case, in order to resolve wave effects the longitudinal panel density over the lifting surface should be 20 panels per wave length or more for panels with constant dipole strength). The local convergence near the leading edge is better than the global one. The distribution of the strength of the leading edge singularity is elliptic like, which vanishes at the free surface and the lower tip.

Cosine spacing near the edges was found to be necessary to account for the lifting effect. An appropriate combination of cosine spacing near the edges and constant spacing in-between may help in obtaining reliable results with limited number of panels.

### Acknowledgments

This study was supported by the Office of Naval Research, contract N00014-88-K-0057.

### References

1. Burton, A.J. and Miller, G.F., *The Application of Integral Equation Methods to the Numerical Solution of Some Exterior Boundary Value Problems*. *Proc. Roy. Soc. Lond. A.* 323, 1971, pp 201-210.
2. Chapman, R.B., *Free Surface Effects for Yawed Surface Piercing Plates*. *J. Ship Res.*, Vol. 20, No. 3, 1976.
3. Daoud, N., *Force and Moments on Asymmetric and Yawed Bodies on a Free Surface*. Ph.D. Thesis, University of California, Berkeley. 1973.
4. Garner, H.C., Hewitt B.L. and Labrujere, T.E., *Comparison of Three Methods for the Evaluation of Subsonic Lifting-Surface Theory*. *Report and Memoranda No. 3597*, June 1968. Aeronautical Research Council, London, England.
5. Lan, C.E., *A Quasi-Vortex-Lattice Method in Thin Wing Theory*. *J. Aircraft*, Vol. 11, No. 9, Sept. 1974
6. Newman, J.N., *Derivation of the Integral Equation for a Rectangular Lifting Surface*. 1961. Unpublished.

7. Newman, J.N., *Evaluation of the Wave Resistance Green Function Part 1. - The Double Integral*, *J. Ship Res.*, Vol.31, No.2, June 1987a, pp 79-90.
8. Newman, J.N., *Evaluation of the Wave Resistance Green Function Part 2. - The Single Integral on the Centerplane*, *J. Ship Res.*, Vol.31, No.3, Sept. 1987b, pp 145-150.
9. Van Den Brug, J.B., Beukelman, W., and Prince, G.J., *Hydrodynamic Forces on a Surface Piercing Flat Plate*. Report No. NR 325, Shipbuilding laboratory, Delft University of Technology. 1971.

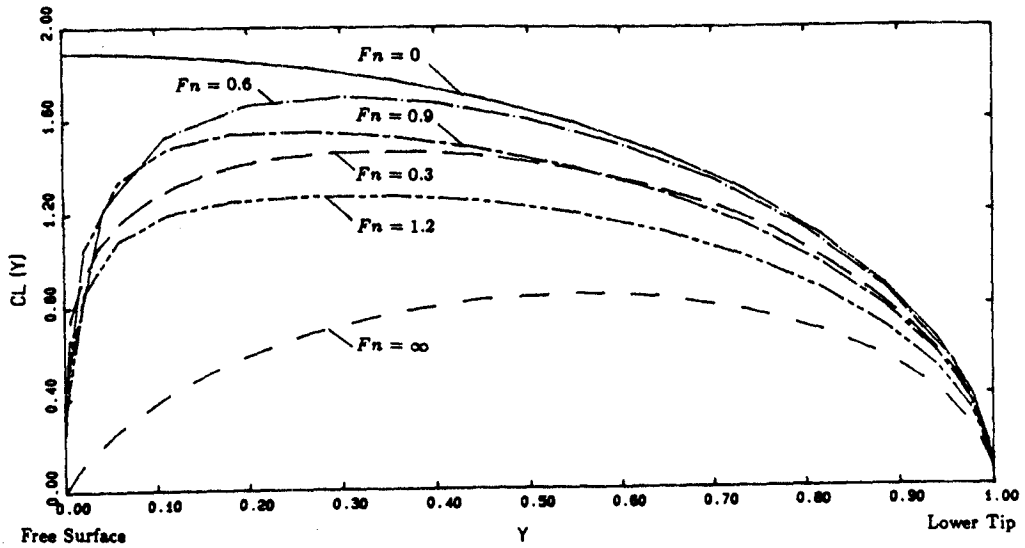


Fig 7. Vertical Lift Coeff. Distributions for Various  $F_n$ .

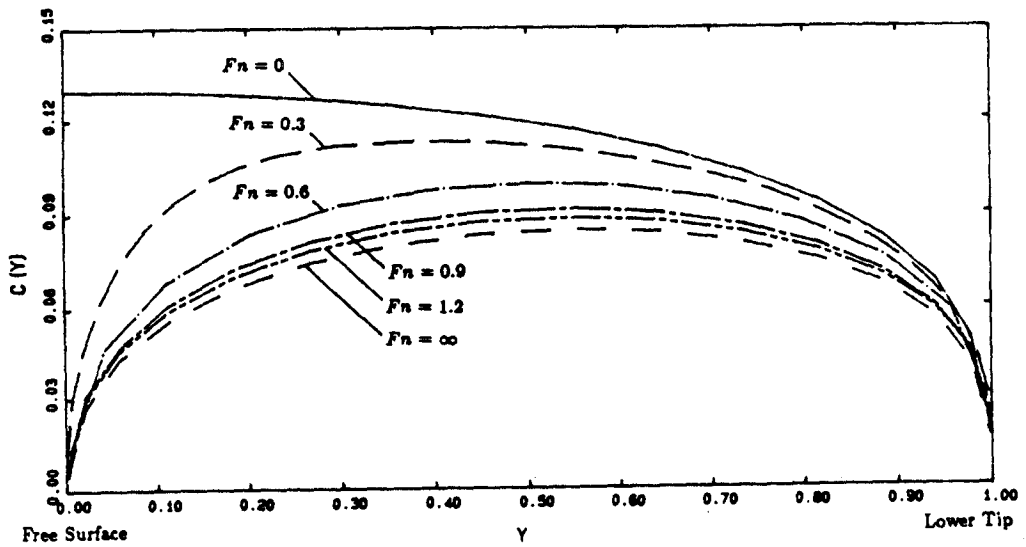


Fig 8. Vertical Distribution of the Strength of L.E. Singularity for Various  $F_n$ .

## DISCUSSION

Tuck: 1) This paper is 91 years overdue! It is the anti-symmetric equivalent of Michell's (symmetric) thin-ship theory, and the authors are to be congratulated for their efforts on a very fundamental and very difficult numerical task. 2) The curve of  $C_L$  versus  $F_n$  seems very jagged at low  $F_n$  and is not continued to the (known?) limit at  $F_n=0$ . It should "obble" like a wave resistance curve (maybe?). Also, what is the graph of (total) drag versus  $F$ ?

Xu & Newman: Thank you Prof. Tuck. As  $F_n$  decreases, the number of panel segments in longitudinal direction increases in proportion to  $F_n$  in order to achieve the same accuracy as in high  $F_n$ . Within the capacity of our VAX 750. We only compute to  $F_n=0.3$ . That's why the  $C_L$  curve didn't continue to the zero  $F_n$  limit which has been calculated. Since we didn't use curve fitting to process the computational results, the  $C_L$  curve appears not so smooth. This may help us to compare the numerical results with the experimental ones. Before we do the computation for  $F_n < 0.3$  it is very hard for us to guess the shape of  $C_L$  curve in that  $F_n$  region.

The total drag  $C_d$  can be easily evaluated in terms of  $C_L$  and  $C_T$  (both are computed) by the following formula:

$$C_d = C_L \alpha - C_T$$

at a given  $F_n$ .

Yeung: In the results you showed in comparison with the experimental measurements of Van den Brug et al. (1971), it appears that satisfactory agreement occurs mostly in the high Froude number regime. Values at more practical Froude number are substantially off. Since Chapman's results are known to do well in the higher Froude number region, perhaps they should also be shown here for comparison purposes and for assessment of the effectiveness of this thin-surface theory.

Xu & Newman: From the results shown it is obvious that the present results predict the trend of  $C_L$  curve ( $C_L$  vs  $F_n$ ) well in the  $F_n$  region as low as  $F_n=0.3$ . This qualitative agreement assures us the convergence of the present scheme. It will be interesting to compare the present results with those reported by Chapman (1976). Since there is no numerical data available in Chapman's paper the comparison between the two approaches was not made. Chapman's approach works well in predicting the global results (e.g.  $C_L$ ,  $C_m$  etc.) but there aren't any results of force distributions available from his paper. Besides, the method he uses doesn't allow one to study the behaviour of the singularity at leading edge which is one of the purposes of the present work.